

Hydrogen dynamics in $\text{Ce}_2\text{Fe}_{17}\text{H}_5$: inelastic and quasielastic neutron scattering studies

A V Skripov¹, N V Mushnikov¹, P B Terent'ev¹, V S Gaviko¹, T J Udovic² and J J Rush^{2,3}

¹ Institute of Metal Physics, Urals Branch of the Academy of Sciences, Ekaterinburg 620990, Russia

² NIST Center for Neutron Research, National Institute of Standards and Technology, Gaithersburg, MD 20899-6102, USA

³ Department of Materials Science and Engineering, University of Maryland, College Park, MD 20742-2115, USA

Received 21 June 2011, in final form 29 July 2011

Published 21 September 2011

Online at stacks.iop.org/JPhysCM/23/405402

Abstract

The vibrational spectrum of hydrogen and the parameters of H jump motion in the rhombohedral $\text{Th}_2\text{Zn}_{17}$ -type compound $\text{Ce}_2\text{Fe}_{17}\text{H}_5$ have been studied by means of inelastic and quasielastic neutron scattering. It is found that hydrogen atoms occupying interstitial Ce_2Fe_2 sites participate in the fast localized jump motion over the hexagons formed by these tetrahedral sites. The H jump rate τ^{-1} of this localized motion is found to change from $3.9 \times 10^9 \text{ s}^{-1}$ at $T = 140 \text{ K}$ to $4.9 \times 10^{11} \text{ s}^{-1}$ at $T = 350 \text{ K}$, and the temperature dependence of τ^{-1} in the range 140–350 K is well described by the Arrhenius law with the activation energy of $103 \pm 3 \text{ meV}$. Our results suggest that the hydrogen jump rate in $\text{Th}_2\text{Zn}_{17}$ -type compounds strongly increases with decreasing nearest-neighbor distance between the tetrahedral sites within the hexagons. Since each such hexagon in $\text{Ce}_2\text{Fe}_{17}\text{H}_5$ is populated by two hydrogen atoms, the jump motions of H atoms on the same hexagon should be correlated.

1. Introduction

Intermetallic compounds R_2Fe_{17} (where R is a rare-earth metal) are known to adopt either the rhombohedral $\text{Th}_2\text{Zn}_{17}$ -type or the hexagonal $\text{Th}_2\text{Ni}_{17}$ -type structure. Hydrogenation of the R_2Fe_{17} compounds leads to a dramatic increase in the Curie temperature and magnetization [1–6], which makes these materials attractive candidates for permanent magnet applications. The structures of the $\text{R}_2\text{Fe}_{17}\text{H}_x$ compounds have been extensively investigated by Isnard *et al* [1, 3, 6]. For materials of both structural types, the host lattice retains its structure after hydrogenation, showing anisotropic expansion with increasing H content. Initially, H atoms in $\text{Th}_2\text{Zn}_{17}$ -type compounds (space group $R\bar{3}m$) fill the distorted octahedral interstitial 9e sites coordinated by four Fe and two R atoms, and at $x = 3$, these sites are fully occupied. Further hydrogenation leads to a partial filling of the tetrahedral interstitial 18g sites coordinated by two Fe and two R atoms. The sublattice of these tetrahedral sites consists of regular hexagons in the basal plane with a side dimension of

$\sim 1.1\text{--}1.2 \text{ \AA}$ (see figure 1). Because of the ‘blocking’ effect [7] originating from a repulsive interaction between H atoms, each 18g-site hexagon can accommodate up to two H atoms, so the maximum occupancy of 18g sites is 1/3. The maximum H content attained experimentally for $\text{Th}_2\text{Zn}_{17}$ -type hydrides $\text{R}_2\text{Fe}_{17}\text{H}_x$ [1–6] is $x = 5$, which corresponds to the complete filling of the 9e sites and a one-third filling of the 18g sites.

While the structural aspects of $\text{Th}_2\text{Zn}_{17}$ -type hydrides $\text{R}_2\text{Fe}_{17}\text{H}_x$ are well understood, little is known about the hydrogen dynamics in these compounds. The only $\text{Th}_2\text{Zn}_{17}$ -type system for which the H dynamics has been investigated in detail is $\text{Pr}_2\text{Fe}_{17}\text{H}_x$ [8–11]. The existence of fast hydrogen jump motion in $\text{Pr}_2\text{Fe}_{17}\text{H}_x$ was first revealed by Mössbauer spectroscopy [8]. Subsequent quasielastic neutron scattering (QENS) experiments [9, 10] gave direct evidence that this fast jump process corresponds to localized H motion over the 18g-site hexagons, whereas H atoms at the 9e sites in $\text{Pr}_2\text{Fe}_{17}\text{H}_x$ remain static on the time scale of the QENS measurements. Such a microscopic picture

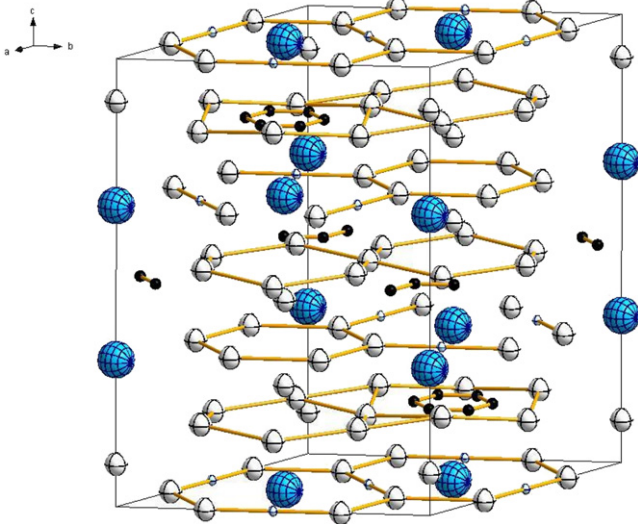


Figure 1. Schematic representation of the rhombohedral $\text{Th}_2\text{Zn}_{17}$ -type structure of $\text{R}_2\text{Fe}_{17}\text{H}_x$ (space group $R\bar{3}m$). Large blue spheres: rare-earth atoms; medium white spheres: Fe atoms; small white spheres: 9e sites; small black spheres: 18g sites. (This figure is in colour only in the electronic version)

of hydrogen motion in $\text{Pr}_2\text{Fe}_{17}\text{H}_x$ is consistent with the structure of the H sublattice in $\text{Th}_2\text{Zn}_{17}$ -type hydrides [1, 3], since the 18g-site hexagons appear to be well separated from each other and from the 9e sites. It should be noted that fast localized motion of H atoms over the hexagons formed by tetrahedral interstitial sites has been extensively studied for Laves-phase hydrides [12–15]. For these compounds, it has been found that the parameters of H jump motion strongly depend on the nearest-neighbor distances between the sites forming the hexagons [15, 16]. In the present work, quasielastic neutron scattering is applied to study the mechanism and parameters of hydrogen jump motion in $\text{Th}_2\text{Zn}_{17}$ -type hydride $\text{Ce}_2\text{Fe}_{17}\text{H}_5$. Since the lattice parameters of $\text{Ce}_2\text{Fe}_{17}\text{H}_5$ are smaller than those of $\text{Pr}_2\text{Fe}_{17}\text{H}_5$ [3], one may expect a significant difference between the H jump rates in these two compounds. The nearest-neighbor distances for the sublattice of the tetrahedral sites also depend on the positional parameters of H atoms at the 18g sites; these parameters may change from one compound to another. QENS experiments in this work are complemented by an inelastic neutron scattering (INS) measurement of the hydrogen vibrational spectrum, which is sensitive to the local environment of H atoms in $\text{Ce}_2\text{Fe}_{17}\text{H}_5$.

2. Experimental details

The intermetallic compound $\text{Ce}_2\text{Fe}_{17}$ was prepared by arc melting in an argon atmosphere followed by annealing in argon at 1000 °C for 72 h. According to x-ray diffraction analysis, the annealed sample was a single-phase compound with the rhombohedral $\text{Th}_2\text{Zn}_{17}$ -type structure (space group $R\bar{3}m$) and the lattice parameters $a = 8.492$ Å and $c =$

12.411 Å. The sample was hydrogenated in a Sieverts-type vacuum system using LaNi_5 hydride as a source of pure hydrogen at a temperature of 463 K and a hydrogen pressure of 16 bar. The host lattice of the hydrogenated sample was found to retain the $\text{Th}_2\text{Zn}_{17}$ -type structure with the lattice parameters $a = 8.665$ Å and $c = 12.581$ Å. These lattice parameters are slightly larger than those reported for $\text{Ce}_2\text{Fe}_{17}\text{H}_{4.8}$ [3] ($a = 8.657$ Å, $c = 12.568$ Å), which is consistent with the gravimetrically estimated H content in our sample (5.0 ± 0.1 H atoms per formula unit).

All neutron scattering experiments were performed at the NIST Center for Neutron Research (Gaithersburg, Maryland, USA). The inelastic neutron scattering measurement of the hydrogen vibrational spectrum at 4 K was made on a filter-analyzer neutron spectrometer (FANS) [17] using the Cu(220) monochromator and horizontal collimations of 20 min of arc before and after the monochromator. The measured range of neutron energy loss was 40–160 meV, and the energy resolution was about 4%–5% of the energy transfer. QENS measurements were performed on the high-flux backscattering spectrometer (HFBS) [18] and on the time-of-flight disk-chopper spectrometer (DCS) [19]. These two spectrometers complement each other with respect to the resolution and the accessible range of energy transfer $\hbar\omega$, enabling one to probe H motion over a range of jump rates from 10^9 to 10^{12} s $^{-1}$. In our experiments, the incident neutron wavelengths λ were 6.27 Å (HFBS), 6.0 and 4.4 Å (DCS), and the energy resolution full widths at half-maximum (FWHM) were 1.0 μeV (HFBS), 67 μeV (DCS, $\lambda = 6.0$ Å) and 170 μeV (DCS, $\lambda = 4.4$ Å). The ranges of elastic momentum transfer $\hbar Q$ studied corresponded to Q ranges of 0.25–1.75 Å $^{-1}$ (HFBS), 0.38–1.75 Å $^{-1}$ (DCS, $\lambda = 6.0$ Å) and 0.49–2.52 Å $^{-1}$ (DCS, $\lambda = 4.4$ Å). The powdered $\text{Ce}_2\text{Fe}_{17}\text{H}_5$ sample was studied in a hollow-cylinder Al container, the sample thickness being 0.3 mm. The sample thickness was chosen to ensure $\sim 90\%$ neutron transmission and thus minimize multiple-scattering effects. In order to determine the temperature range where the effects of quasielastic line broadening become observable on the energy scale of the backscattering spectrometer, we used a fixed-window operation mode of the HFBS. In this mode, the Doppler drive is stopped (so the energy transfer is zero), and the elastic scattering intensity at different Q values is recorded as a function of temperature. For such an elastic scan, the sample temperature was swept from 290 to 4 K at a rate of 1 K min $^{-1}$. QENS spectra were recorded at $T = 4, 140, 160, 180$ and 210 K on HFBS, at $T = 30, 240, 265, 290$ and 320 K on DCS with $\lambda = 6.0$ Å, and at $T = 30$ and 350 K on DCS with $\lambda = 4.4$ Å. For the analysis of the DCS data, the detectors were binned into nine groups. The scattering angles corresponding to the Bragg reflections were excluded from the analysis. The instrumental resolution functions were determined from the measured QENS spectra for $\text{Ce}_2\text{Fe}_{17}\text{H}_5$ at low temperatures (4 K for HFBS and 30 K for DCS). It should be noted that, throughout the figures in this paper, vertical error bars denote one standard deviation. Where no error bars are shown, the uncertainties are commensurate with the observed scatter in the data.

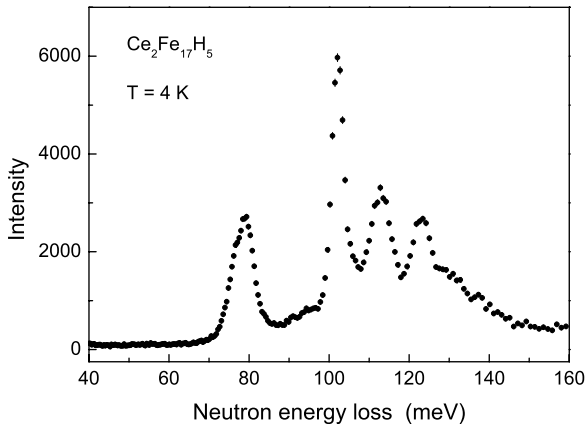


Figure 2. The 4 K inelastic neutron scattering spectrum for $\text{Ce}_2\text{Fe}_{17}\text{H}_5$.

3. Results and discussion

3.1. Neutron vibrational spectroscopy

The experimental low-temperature INS spectrum for $\text{Ce}_2\text{Fe}_{17}\text{H}_5$ is shown in figure 2. This spectrum consists of four well-resolved main peaks centered at ~ 79 , 102, 113 and 123 meV. For comparison, the low-temperature INS spectrum reported for $\text{Pr}_2\text{Fe}_{17}\text{H}_5$ [9, 11] consists of three well-resolved peaks centered at ~ 75 , 105 and 124 meV, and a ‘shoulder’ at ~ 112 meV. For metal–hydrogen systems, INS spectra in the energy transfer range 50–160 meV are usually dominated by the fundamental modes of H optical vibrations. The simplest approach to the description of these vibrations is based on the model of a three-dimensional Einstein oscillator [20, 21]. For the $\hbar\omega$ range of fundamental modes, this model predicts three peaks of nearly equal intensity. Depending on the point symmetry of H sites, all or two of these peaks may be degenerate. For hydrogen in both the 9e and 18g sites of $\text{Th}_2\text{Zn}_{17}$ -type compounds, the local symmetry is lower than axial; therefore, one may generally expect three peaks from each of these sites.

On the basis of the previous analysis for $\text{Pr}_2\text{Fe}_{17}\text{H}_x$ [11], we can safely ascribe the low-energy peaks at 79 and 102 meV to hydrogen at octahedral 9e sites in $\text{Ce}_2\text{Fe}_{17}\text{H}_5$. Indeed, similar low-energy peaks were found to survive when the H content in $\text{Pr}_2\text{Fe}_{17}\text{H}_x$ was reduced from $x = 5$ to 3 [11]. Each H atom at 9e sites in $\text{Ce}_2\text{Fe}_{17}\text{H}_5$ is coordinated with two Ce atoms at the distance $r_{\text{eR}} = 2.49$ Å (in the basal plane), two Fe atoms at $r_{\text{eFe1}} = 1.87$ Å (in the basal plane) and two Fe atoms at $r_{\text{eFe2}} = 1.94$ Å (along the c axis) [1]. Following the arguments of [11], the low-energy peak at 79 meV should be attributed to H vibrations along the c axis, since the corresponding H–Fe distance r_{eFe2} is longer than r_{eFe1} . The stronger peak at 102 meV is then assigned to H vibrations in the basal plane with nearly the same energies. Note that the energy difference between the two peaks originating from hydrogen at octahedral 9e sites in $\text{Ce}_2\text{Fe}_{17}\text{H}_5$ (23 meV) is smaller than the corresponding difference in $\text{Pr}_2\text{Fe}_{17}\text{H}_5$ (30 meV [11]). This is consistent with the fact that the

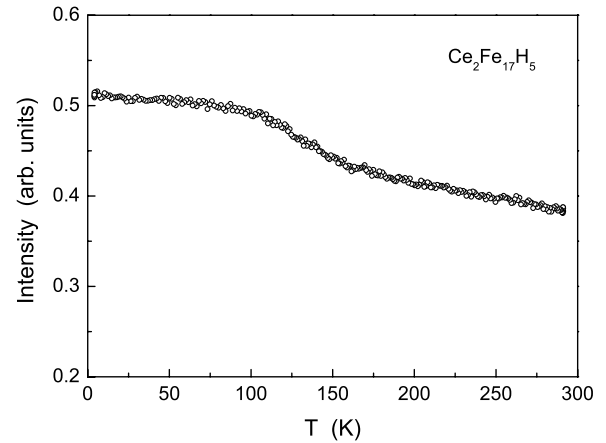


Figure 3. The temperature dependence of the elastic scattering intensity for $\text{Ce}_2\text{Fe}_{17}\text{H}_5$ measured over the Q range $0.99\text{--}1.68$ Å $^{-1}$ using the fixed-window operation mode of HFBS.

difference between the distances r_{eFe2} and r_{eFe1} in $\text{Ce}_2\text{Fe}_{17}\text{H}_5$ (0.07 Å) is smaller than that in $\text{Pr}_2\text{Fe}_{17}\text{H}_5$ (~ 0.1 Å [11]).

The peaks centered at 113 and 123 meV (figure 2) can be assigned to two of the three expected normal modes of H atoms at tetrahedral 18g sites. The increased energies of these modes are consistent with the smaller size of the tetrahedral sites, as compared to the octahedral sites. These two peaks in $\text{Ce}_2\text{Fe}_{17}\text{H}_5$ are observed at nearly the same energies as in $\text{Pr}_2\text{Fe}_{17}\text{H}_5$; however, for $\text{Pr}_2\text{Fe}_{17}\text{H}_5$ the feature at ~ 112 meV appears just as a ‘shoulder’ of the strongest peak due to H at 9e sites. The third peak expected for vibrations of H atoms at 18g sites is most probably hidden [11] beneath this strongest peak.

3.2. Quasielastic neutron scattering

Figure 3 shows the temperature dependence of the elastic scattering intensity measured over the Q range $0.99\text{--}1.68$ Å $^{-1}$ using the fixed-window operation mode of HFBS. As can be seen from this figure, the results of the elastic scan exhibit a characteristic step in the range 120–180 K. The amplitude of the observed changes in the relative elastic scattering intensity considerably exceeds that expected for the temperature dependence of the Debye–Waller factor. Therefore, the elastic intensity drop in the range 120–180 K suggests quasielastic line broadening due to the onset of H jump motion on the time scale corresponding to the HFBS resolution. These results indicate that the changes in QENS spectra measured by HFBS should be most pronounced within the T range of the step.

Consistent with the elastic scan results, quasielastic line broadening has been observed for the spectra measured on HFBS at $T \geq 140$ K. These QENS spectra can be satisfactorily described by a sum of two components: a narrow ‘elastic’ line represented by the spectrometer resolution function $R(Q, \omega)$ and a resolution-broadened Lorentzian ‘quasielastic’ line. Figure 4 shows, as an example of the data, the QENS spectrum measured on HFBS at $T = 180$ K and $Q = 1.68$ Å $^{-1}$. The

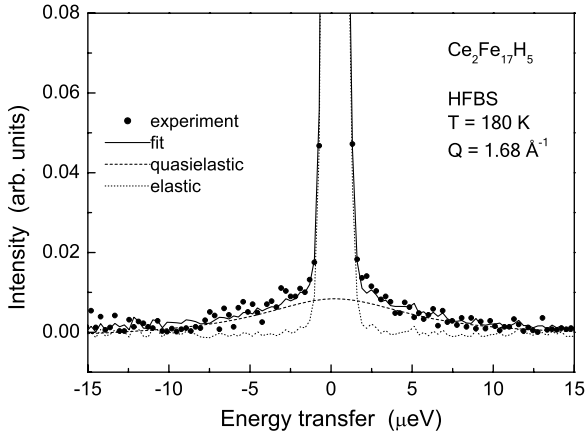


Figure 4. The QENS spectrum for $\text{Ce}_2\text{Fe}_{17}\text{H}_5$ measured on HFBS at $T = 180 \text{ K}$ and $Q = 1.68 \text{ \AA}^{-1}$. The energy transfer channels are binned in groups of three. The full curve shows the fit of the two-component model (equation (1)) to the data. The dotted curve represents the elastic component (the spectrometer resolution function), and the dashed curve shows the Lorentzian quasielastic component.

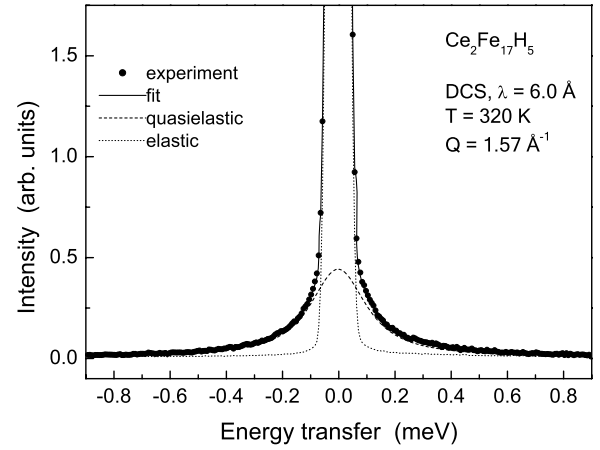


Figure 5. The QENS spectrum for $\text{Ce}_2\text{Fe}_{17}\text{H}_5$ measured on DCS ($\lambda = 6.0 \text{ \AA}$) at $T = 320 \text{ K}$ and $Q = 1.57 \text{ \AA}^{-1}$. The circles are the experimental points interpolated to the uniform energy grid. The full curve shows the fit of the two-component model (equation (1)) to the data. The dotted curve represents the elastic component (the spectrometer resolution function), and the dashed curve shows the Lorentzian quasielastic component.

width of the quasielastic component increases with increasing temperature, and at $T > 210 \text{ K}$ it exceeds the energy transfer range of $\pm 35 \text{ \mu eV}$ probed by HFBS. Therefore, at higher temperatures, a time-of-flight neutron spectrometer is required to obtain the parameters of H jump motion. The QENS spectra measured on DCS in the range 240–350 K can also be described by a sum of the elastic line and the broader Lorentzian component. Figure 5 shows, as an example of the data, the QENS spectrum measured on DCS ($\lambda = 6.0 \text{ \AA}$) at $T = 320 \text{ K}$ and $Q = 1.57 \text{ \AA}^{-1}$. All the spectra have been fitted with the model incoherent scattering function

$$S_{\text{inc}}(Q, \omega) = A_0(Q)\delta(\omega) + [1 - A_0(Q)]L(\omega, \Gamma) \quad (1)$$

convoluted with $R(Q, \omega)$. Here $\delta(\omega)$ is the elastic δ -function, $L(\omega, \Gamma)$ is the quasielastic Lorentzian function with the half-width at half-maximum Γ , and A_0 is the weight of the elastic component. The solid curves in figures 4 and 5 show the fits of this two-component model to the data, and the broken curves represent contributions of the two components. At all of the temperatures studied, the half-width Γ of the quasielastic component is found to be nearly Q independent. Such a behavior is typical of a spatially confined (localized) atomic motion [22, 23]. Therefore, the observed QENS spectra can be attributed to a fast localized H motion with the jump rate τ^{-1} . In this case, the value of Γ should be proportional to τ^{-1} , while the Q dependence of the elastic incoherent structure factor (EISF), A_0 , should be related to the geometry of this motion.

At the next stage of the analysis, the values of Γ were fixed to their average values at a given temperature, and the Q dependence of A_0 was derived from the fits of the two-component model (equation (1)) to the data. In order to obtain the EISF for the hydrogen sublattice, the resulting A_0 values were corrected for the small Q -independent elastic contribution of the host-metal lattice. Figure 6 shows the Q dependences of the EISF for the H sublattice at three

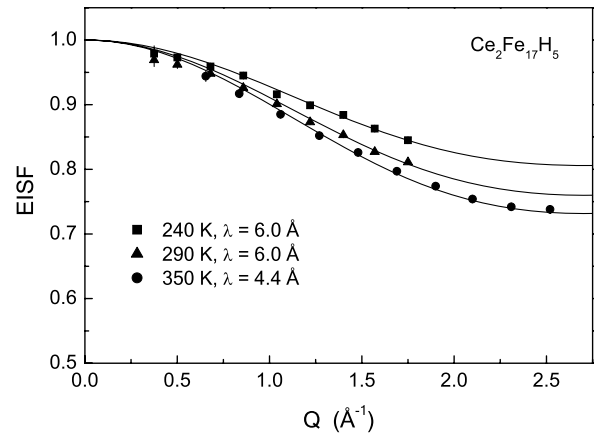


Figure 6. The EISF for the hydrogen sublattice in $\text{Ce}_2\text{Fe}_{17}\text{H}_5$ as a function of Q at $T = 240, 290,$ and 350 K . The full curves show the fits of the six-site model (equation (2)) with fixed $r = 1.08 \text{ \AA}$ to the data.

temperatures. For the measurements at other temperatures, the Q dependences of the EISF have similar shapes. As can be seen from figure 6, the measured EISF is temperature dependent, decreasing with increasing T . This feature is common to all the Laves-phase hydrides studied [12, 13, 15, 24] and $\text{Pr}_2\text{Fe}_{17}\text{H}_x$ [9, 10]; it can be accounted for in terms of a temperature-dependent fraction of H atoms participating in the localized motion on the time scale of the QENS measurements [12, 15]. First, we have to verify whether the observed Q dependence of the EISF in $\text{Ce}_2\text{Fe}_{17}\text{H}_5$ is consistent with H jump motion over the hexagons formed by the 18g sites. Since the distance between the nearest-neighbor 18g sites in $\text{Ce}_2\text{Fe}_{17}\text{H}_5$, $r_{\text{gg}} = 1.08 \text{ \AA}$, is considerably shorter than the distances both between the nearest-neighbor 9e sites, $r_{\text{ee}} = 4.33 \text{ \AA}$, and between the nearest-neighbor 9e and 18g sites, $r_{\text{eg}} = 2.66 \text{ \AA}$ [1], it is reasonable to assume that H atoms at the octahedral 9e sites (3/5 of all H

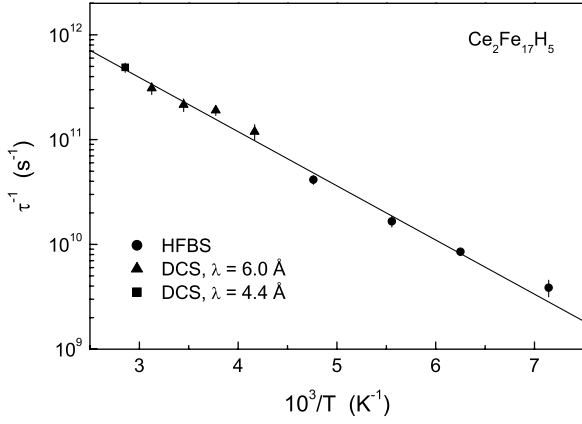


Figure 7. The hydrogen jump rate as a function of the inverse temperature for $\text{Ce}_2\text{Fe}_{17}\text{H}_5$. The full line shows the Arrhenius fit to the data obtained on both HFBS and DCS.

atoms in $\text{Ce}_2\text{Fe}_{17}\text{H}_5$) are immobile on the time scale of our measurements. Assuming further that only a fraction p of H atoms in the tetrahedral 18g sites participate in the fast localized motion, we can write the orientationally averaged EISF for the model of jumps between six equidistant sites on a circle of radius r [22, 23] in the form

$$A_0(Q) = 1 - \frac{2p}{5} + \frac{p}{15} \times [1 + 2j_0(Qr) + 2j_0(Qr\sqrt{3}) + j_0(2Qr)], \quad (2)$$

where $j_0(x)$ is the spherical Bessel function of zeroth order. The fit of this six-site model (equation (2)) to the data at $T = 350$ K (corresponding to the strongest variation of the EISF) yields $p = 0.72 \pm 0.03$ and $r = 1.13 \pm 0.06$ Å. Since the fitted value of r is close to the value $r_{\text{gg}} = 1.08$ Å derived from the refinement of neutron diffraction data for $\text{Ce}_2\text{Fe}_{17}\text{H}_{4.8}$ [1], we can conclude that the observed Q dependence of the EISF is consistent with H jump motion over the hexagons formed by the tetrahedral 18g sites. By fixing the value of r to $r_{\text{gg}} = 1.08$ Å, we have found satisfactory fits of the six-site model (equation (2)) to the data at all of the temperatures studied with p as the only fit parameter. The results of these fits are shown by solid curves in figure 6. The behavior of p resulting from these fits will be discussed below.

In order to determine the jump rate of the localized H motion, τ^{-1} , we have to consider a relation between Γ and τ^{-1} . A rigorous description in terms of the six-site model [22] suggests that the quasielastic component of the QENS spectrum is a sum of three Lorentzian lines with the half-widths $0.5\hbar\tau^{-1}$, $1.5\hbar\tau^{-1}$ and $2\hbar\tau^{-1}$, and Q -dependent amplitudes. However, at $Qr < 2$ (which corresponds to the experimental Q range for most of our measurements) this sum is strongly dominated by the Lorentzian with the half-width of $0.5\hbar\tau^{-1}$ [22]. As has been noted previously [12, 25], because of the limited experimental accuracy, it is practically impossible to distinguish between such a three-component quasielastic line and a single Lorentzian with a Q -independent width. We have adopted the simplified description based on a single Lorentzian with $\Gamma \approx 0.55\hbar\tau^{-1}$ [22]; such a description is very close to the rigorous one at $Qr < 2$. The resulting

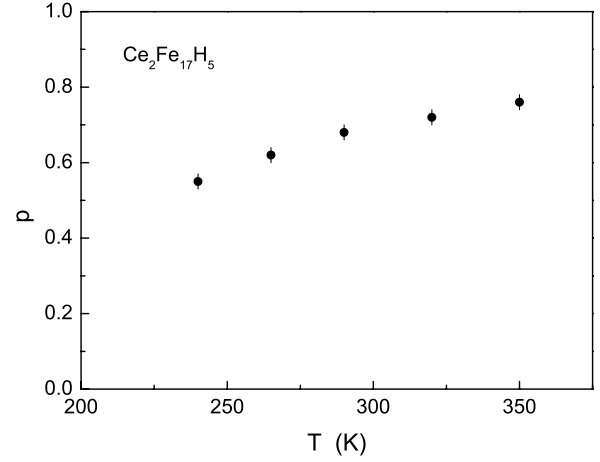


Figure 8. The temperature dependence of the fraction of H atoms in 18g sites participating in the fast localized motion.

temperature dependence of the H jump rate τ^{-1} is shown in figure 7. It can be seen from this figure that a combination of the backscattering and time-of-flight QENS data allows us to probe the changes in τ^{-1} over a range of nearly two orders of magnitude. The temperature dependence of τ^{-1} can be satisfactorily described by the Arrhenius law,

$$\tau^{-1} = \tau_0^{-1} \exp(-E_a/k_B T), \quad (3)$$

where E_a is the activation energy for the localized H motion. The solid line in figure 7 shows the Arrhenius fit to the $\tau^{-1}(T)$ data; the corresponding fit parameters are $\tau_0^{-1} = (1.4 \pm 0.4) \times 10^{13} \text{ s}^{-1}$ and $E_a = 103 \pm 3$ meV. It should be noted that the localized H motion in $\text{Ce}_2\text{Fe}_{17}\text{H}_5$ is considerably faster than in $\text{Pr}_2\text{Fe}_{17}\text{H}_5$. For example, at 200 K, the hydrogen jump rate in $\text{Ce}_2\text{Fe}_{17}\text{H}_5$ is about fivefold higher than that found in $\text{Pr}_2\text{Fe}_{17}\text{H}_5$ [9]. The activation energy for H jump motion in $\text{Ce}_2\text{Fe}_{17}\text{H}_5$ is lower than in $\text{Pr}_2\text{Fe}_{17}\text{H}_5$ (140 meV [9]). These results indicate that, as in the case of Laves-phase hydrides [15, 16], the hydrogen jump rates in $\text{R}_2\text{Fe}_{17}\text{H}_x$ are very sensitive to changes in the nearest-neighbor distances r_{gg} within the g-site hexagons. In fact, the change in the r_{gg} value from 1.16 Å for $\text{Pr}_2\text{Fe}_{17}\text{H}_5$ [9] to 1.08 Å for $\text{Ce}_2\text{Fe}_{17}\text{H}_5$ results in a strong increase in the H jump rate and a substantial decrease in the activation energy.

We now turn to a discussion of the temperature-dependent fraction p of H atoms participating in the localized motion over the g-site hexagons. The temperature dependence of p resulting from the fits of equation (2) to the DCS data is shown in figure 8. As can be seen from this figure, the value of p slowly increases with T , approaching 0.8 at the highest temperature of our measurements. Similar behavior of p was found for $\text{Pr}_2\text{Fe}_{17}\text{H}_x$ [9, 10]. The increase in p with increasing T was also observed for localized H motion in Laves-phase hydrides [12, 13, 15, 24], α - ScH_x [26], and α - LaNi_5H_x [25]; in these cases, the presence of the immobile fraction $1 - p$ was attributed to H–H interactions leading to the formation of some ordered H configurations, which are destroyed at higher temperatures due to thermal fluctuations. For Laves-phase hydrides, this interpretation is supported by the observed

decrease in the value of p with increasing H concentration [12, 27]. However, such an interpretation cannot be extended to the case of $R_2Fe_{17}H_5$, where each g-site hexagon is occupied by two H atoms. In fact, due to the ‘blocking’ effect [7], two H atoms can only occupy the opposite vertices on each g-site hexagon. In such a configuration, two H atoms are expected to block each other’s random jumps over the hexagon. Therefore, the motion of two H atoms on the same hexagon should be correlated, as if they formed a bound pair. The presence of such correlations does not affect the validity of equation (2), since in our case the observed neutron scattering is dominated by the incoherent contribution, and the EISF is determined by the set of sites visited by an individual H atom [22, 23]. In the case of $Pr_2Fe_{17}H_x$, it was found [10] that the values of p for compounds with $x = 5$ and 4 are nearly the same. Thus, removing one-half of the hydrogen atoms from the 18g sites does not lead to any significant increase in the fraction of mobile H atoms. This result suggests that the immobilization of some H atoms at the 18g sites occurs due to defects in the host-metal lattice rather than H–H interactions. Note that an increase in the fraction of immobile H atoms with increasing level of lattice distortions has been reported for the ball-milled Laves-phase system $ZrCr_2H_3$ [27]. Host-lattice distortions are expected to distort the g-site hexagons, making some of them unsuitable for the fast localized H motion.

An alternative approach to the description of the temperature-dependent EISF is based on the model of jumps between inequivalent positions. For this model, all H atoms occupying the 18g sites are expected to participate in the localized motion, but the occupancy probabilities of different sites on a hexagon are not equal to each other. Such a model is naturally related to host-metal lattice defects that can cause a distribution of the potential well depths at the 18g sites. As in the case of the immobile fraction of H atoms, the model of jumps between inequivalent sites is known to result in a larger EISF [22], compared to jumps between equivalent sites. The temperature dependence of the EISF can then be attributed to changes in the occupancy probabilities of different sites. However, the Q dependence of the EISF prevents us from distinguishing between the models based on the immobile fraction of H atoms and on jumps over inequivalent positions.

4. Conclusions

The results of our neutron vibrational spectroscopy measurements for $Ce_2Fe_{17}H_5$ are consistent with the locations of hydrogen atoms determined from earlier diffraction data: three H atoms per formula unit fully occupy the distorted octahedral 9e sites of the host lattice, while two H atoms per formula unit fill one-third of the tetrahedral 18g sites. The analysis of our quasielastic neutron scattering data for $Ce_2Fe_{17}H_5$ has shown that H atoms occupying the 18g sites participate in the fast localized motion over the hexagons formed by these sites. The fraction of mobile H atoms in these sites increases with temperature. The hydrogen jump rate τ^{-1} of this localized motion is found to change from $3.9 \times 10^9 \text{ s}^{-1}$ at 140 K to $4.9 \times 10^{11} \text{ s}^{-1}$ at 350 K, and the temperature dependence of τ^{-1} in the range 140–350 K

is well described by the Arrhenius law with the activation energy $E_a = 103 \pm 3 \text{ meV}$. The values of τ^{-1} for $Ce_2Fe_{17}H_5$ are considerably higher than those for the previously studied $Pr_2Fe_{17}H_5$ [9]; this result indicates that the H jump rates in Th_2Zn_{17} -type compounds are very sensitive to changes in the nearest-neighbor distance r_{gg} within the 18g-site hexagons. Because of the repulsive H–H interaction, two hydrogen atoms at each 18g-site hexagon can only occupy the opposite vertices. Therefore, the jump motion of two H atoms on the same hexagon should be correlated, as if they formed a bound pair. Direct evidence of the correlated motion can, in principle, be obtained from studies of the coherent contribution to the neutron scattering; such experiments would require deuterated samples or the use of spin-polarized neutrons. It would also be interesting to compare the details of H jump motion in $R_2Fe_{17}H_x$ compounds with one and two H atoms at each hexagon formed by the tetrahedral sites. One possibility is studying $R_2Fe_{17}H_x$ compounds with heavier rare-earth elements for which the maximum attainable H concentration is close to $x = 4$ [3]. These experiments are planned for the near future.

Acknowledgments

This work utilized facilities supported in part by the National Science Foundation under Agreement no. DMR-0454672. This work was also supported by the Priority Program ‘Basics of Development of Energy Systems and Technologies’ of the Russian Academy of Sciences. AVS acknowledges financial support from the NIST Center for Neutron Research.

References

- [1] Isnard O, Miraglia S, Soubeyrou J L, Fruchart D and Stergion A 1990 *J. Less-Common Met.* **162** 273
- [2] Isnard O, Miraglia S, Fruchart D and Deportes J 1992 *J. Magn. Magn. Mater.* **103** 157
- [3] Isnard O, Miraglia S, Soubeyrou J L, Fruchart D and L’Héritier P 1994 *J. Magn. Magn. Mater.* **137** 151
- [4] Isnard O, Miraglia S, Fruchart D, Giorgetti C, Pizzini S, Dartyge E, Krill G and Kappler J P 1994 *Phys. Rev. B* **49** 15692
- [5] Fujii H, Akayama M, Nakao K and Tatami K 1995 *J. Alloys Compounds* **219** 10
- [6] Isnard O, Miraglia S, Fruchart D, Akiba E and Nomura K 1997 *J. Alloys Compounds* **257** 150
- [7] Switendick A C 1979 *Z. Phys. Chem. N. F.* **117** 89
- [8] Hautot D, Long G J, Grandjean F, Isnard O and Miraglia S 1999 *J. Appl. Phys.* **86** 2200
- [9] Mamontov E, Udovic T J, Isnard O and Rush J J 2004 *Phys. Rev. B* **70** 214305
- [10] Mamontov E, Udovic T J, Rush J J and Isnard O 2006 *J. Alloys Compounds* **422** 149
- [11] Udovic T J, Zhou W, Wu H, Brown C M, Rush J J, Yildirim T, Mamontov E and Isnard O 2007 *J. Alloys Compounds* **446/447** 504
- [12] Skripov A V, Cook J C, Sibirtsev D S, Karmonik C and Hempelmann R 1998 *J. Phys.: Condens. Matter* **10** 1787
- [13] Skripov A V, Cook J C, Udovic T J and Kozhanov V N 2000 *Phys. Rev. B* **62** 14099
- [14] Bull D J, Broom D P and Ross D K 2003 *Chem. Phys.* **292** 253
- [15] Skripov A V 2003 *Defect Diffus. Forum* **224/225** 75

- [16] Skripov A V 2005 *J. Alloys Compounds* **404–406** 224
- [17] Udovic T J *et al* 2008 *Nucl. Instrum. Methods A* **588** 406
- [18] Meyer A, Dimeo R M, Gehring P M and Neumann D A 2003 *Rev. Sci. Instrum.* **74** 2759
- [19] Copley J R D and Cook J C 2003 *Chem. Phys.* **292** 477
- [20] Richter D, Hempelmann R and Bowman R C 1992 *Hydrogen in Intermetallic Compounds II* ed L Schlapbach (Berlin: Springer) p 97
- [21] Ross D K 1997 *Hydrogen in Metals III* ed H Wipf (Berlin: Springer) p 153
- [22] Bée M 1988 *Quasielastic Neutron Scattering* (Bristol: Hilger)
- [23] Hempelmann R 2000 *Quasielastic Neutron Scattering and Solid State Diffusion* (Oxford: Clarendon)
- [24] Skripov A V, Udovic T J and Rush J J 2007 *Phys. Rev. B* **76** 104305
- [25] Schönfeld C, Hempelmann R, Richter D, Springer T, Dianoux A J, Rush J J, Udovic T J and Bennington S M 1994 *Phys. Rev. B* **50** 853
- [26] Berk N F, Rush J J, Udovic T J and Anderson I S 1991 *J. Less-Common Met.* **172–174** 496
- [27] Skripov A V, Udovic T J, Rush J J and Uimin M A 2011 *J. Phys.: Condens. Matter* **23** 065402